Extracting the Invisible: Mesial Temporal Source Detection in Simultaneous EEG and SEEG Recordings

Eric Ternisien
Université de lorraine
Thierry Cecchin
Université de Lorraine, CNRS, CRAN
Sophie Colnat-Coulbois
Université de Lorraine, CNRS, CRAN
Louis Georges Maillard
Université de Lorraine, CNRS, CRAN
Laurent Koessler (laurent.koessler@univ-lorraine.fr)
Université de Lorraine, CNRS, CRAN

Research Article

Keywords: blind source separation, deep brain sources, epileptic discharges, mesial temporal lobe epilepsy, simultaneous EEG-SEEG recordings, kurtosis

Posted Date: November 1st, 2022

DOI: https://doi.org/10.21203/rs.3.rs-2201044/v1

Additional Declarations: No competing interests reported.

Version of Record: A version of this preprint was published at Brain Topography on February 2nd, 2023. See the published version at https://doi.org/10.1007/s10548-023-00940-5.

Abstract

Epileptic source detection relies mainly on visual expertise of scalp EEG signals, but it is recognised that epileptic discharges can escape to this expertise due to a deep localization of the brain sources that induce a very low, even negative, signal to noise ratio. In this methodological study, we aimed at automatically extract deep mesial temporal sources that were invisible in scalp EEG signals using blind source separation (BSS) methods (infomax ICA, extended infomax ICA, and JADE) combined with a statistical measure (kurtosis). We estimated the effect of different methodological and physiological parameters that could alter or improve the automatic extraction. Using nine well-defined mesial epileptic networks (1,949 spikes) obtained from seven patients and simultaneous EEG-SEEG recordings, the first independent component extracted from the scalp EEG signals was validated in mean from 46–80% according to the different parameters. The three BSS methods equally performed (no significant difference) and no influence of the number of scalp electrodes used was found. At the opposite, the number and amplitude of spikes included in the averaging before the extraction modified the performance. Anyway, despite their invisibility in scalp EEG signals, this study demonstrates that deep source extraction is feasible under certain conditions and with the use of common signal analysis toolboxes. This finding confirms the crucial need to continue the signal analysis of scalp EEG recordings for extracting new electrophysiological biomarkers.

Introduction

Few recent studies using simultaneous multi-scale electroencephalography (EEG) recordings demonstrated that deep brain sources contribute to scalp EEG recordings but are not spontaneously visible by visual expertise (Koessler et al. 2015; Ramantani et al. 2016; Pyrzowski et al. 2021; Lee et al. 2021). These brain sources, despite their depth and their mixing activity with superficial sources, can generate electric field potentials that project on scalp electrodes with a low signal to noise ratio (SNR). Extracting these EEG potentials from the deep mesial temporal sources would be very crucial because they could be used as biomarkers of pathological (e.g., epilepsy or Alzheimer disease) or cognitive (e.g., memory, language, and sleep in particular) processes. The lack of awareness of these biomarkers can induce misinterpretation, wrong medical treatment strategies or the use of invasive recordings in clinical context such as drug resistant epilepsy.

Applied to EEG (or magnetoencephalography, MEG), blind source separation (BSS) approach is an interesting method to suppress environmental or physiological EEG artefacts but also to identify and separate brain sources from EEG recordings (Jung et al. 2001; Jutten and Karhunen 2004; Congedo et al. 2008). This automatic and unsupervised (i.e., without visual expertise) method could be used to extract deep brain sources from scalp EEG signals. In 2019, Pizzo and colleagues used BSS, and especially an independent component analysis (ICA) method, to disentangle the activity from focal deep and large superficial brain sources from MEG signals and using stereoelectroencephalographic (SEEG) recordings as reference method. They noticed that large band-pass filtering (2–60 Hz) and high number of events to average result are required to increase visibility of independent components (ICs). Hippocampal and amygdala activations could be found in 6 out of 14 patients and from some patients (4 out of 14) ICA revealed evidence of a thalamic signal. This promising result relies on an advanced technology (i.e., MEG) and on the use of a high number of sensors (248 magnetometers). Because MEG technology cannot be commonly used in a high number of clinical or research centres, BSS approach for deep sources detection need to be investigated with scalp EEG that is the most common, portable and easy to use electrophysiological technique. This investigation should be particularly important and informative especially in a scalp EEG context with low spatial resolution (10/20 system; Seeck et al. 2017) and a resistive volume conduction (especially the skull; Akhtari et al. 2002) context that reduce the SNR (at the difference to MEG where magnetic fields flow without attenuation in the head tissues).

In this paper, the first aim was to evaluate the efficiency of different BSS methods, combined with a statistical measure (Kurtosis), to extract automatically deep brain sources from scalp EEG recordings using a well-defined simultaneous EEG-SEEG dataset of mesial deep temporal sources (Koessler et al. 2015). The second aims were to investigate the influence of methodological and physiological parameters that could alter or improve the automatic extraction. For methodological parameters, we evaluated the influence of the independent component ranks and the number of scalp EEG electrodes. For the physiological parameters, we evaluated the influence of the amplitude of the brain sources and the number of averaged interictal events. At the end, we identified the causes of non-detection and proposed an improvement of the method using an expert control.

Materials & Methods

Patients and dataset

Patients

For this study, we used nine simultaneous EEG-SEEG datasets corresponding to mesial networks from a previous investigation (Koessler et al. 2015) involving seven patients (three females, mean age of 38 years) with temporal lobe epilepsy (TLE). These patients had (i) an epileptogenic zone confined to the temporal lobe and (ii) at least one interictal intracerebral spike (IIS) source confined to the mesial temporal lobe (MTL), as defined by SEEG recordings. All included patients agreed to participate in this study, approved by the ethical committee of our institution (CHRU, Nancy), and the database has been declared to the CNIL.

Simultaneous EEG-SEEG recordings

Simultaneous SEEG and EEG recordings were performed using a 128-channel system with 512 Hz sample rate and scalp FPz electrode as reference. For all patients, the following brain structures were sampled with multi-contact SEEG electrodes: amygdala; anterior and posterior hippocampus; entorhinal cortex; collateral fissure; parahippocampal gyrus; internal and external temporal pole; superior, middle, and inferior temporal gyri; temporo-occipital junction; fusiform gyrus; insula. Further SEEG electrodes were occasionally placed according to the spatial distribution of interictal spikes and the respective electroclinical hypothesis. For scalp EEG recordings, two main scalp regions were sampled: the fronto-centro-parietal region and the lateral and basal temporal regions ipsi-

and contralateral to the presumed epileptogenic zone. Two to three hours of EEG-SEEG recordings during calm wakefulness are selected for interictal spike analysis, avoiding ictal events or preictal changes.

Dataset pre-processing

All data analyses were performed using Matlab software (MATLAB 7.0, The MathWorks, Inc.) and, for BSS, the toolbox EEGLAB (Delorme and Makeig 2004). Data pre-processing included three consecutive steps: IIS selection, IIS network classification and averaged ISS extraction. These steps are described below.

IIS selection

First, SEEG recordings were visually analysed using a bipolar montage. IIS networks were defined by the reproducible co-occurrence of IIS in different temporal lobe structures. These IIS networks were classified as: mesial (M) if IIS co-occurred within the MTL comprising the amygdala, hippocampus, entorhinal cortex, parahippocampal gyrus and collateral sulcus; neocortical (NC) if IIS co-occurred within any other temporal neocortical structures lateral to the collateral sulcus (fusiform, inferior, middle, and superior temporal gyri) and mesial plus neocortical (M + NC) if IIS co-occurred within both MTL and neocortical structures. Within each of these networks, the source corresponding to the earliest IIS with the highest amplitude was considered as the principal source of the network. These IIS were manually marked with a trigger (t_0) at the peak of the initial component, then segments of 1 sec centred on the local extreme t_0 were automatically extracted and the corresponding amplitude and latency computed.

Second, condensed cartographies of IIS amplitude and latency were obtained for each network in order to (i) ascertain that the selected IIS was indeed the earliest event with the highest amplitude within the network, and to (ii) verify that all individual spikes presented an identical intracerebral distribution and therefore belonged to the same network.

Lastly, to check that non-mesial SEEG contacts were not activated at t_0, a quantitative validation was performed. Each IIS was compared to background activity, in every SEEG contact, by a statistical test of outlier rejection under the null hypothesis that the amplitude of the peak did not significantly differ from the amplitude of the background activity as measured in the intervals [-500, -250] and [250,500] ms around t_0.

IIS network classification

Condensed cartographies with similar IIS distribution were concatenated and classified using visual expert and statistical analysis into one of three distinct categories: (i) M if IIS were recorded only within mesial temporal structures; (ii) NC if IIS were recorded in structures lateral to the collateral fissure; (iii) M + NC if IIS were recorded simultaneously or within a maximum latency of 20 ms in both mesial and neocortical temporal structures.

Averaged ISS extraction

Scalp EEG segments were extracted using the same 1 sec epoch centred on t_0 as SEEG segments. Segments with scalp EEG amplitude > 150 µV that represented < 10% of all segments were rejected and considered as artifacts. The remaining segments were band-pass filtered (1.5–30 Hz) and averaged.

Blind source separation and independent components validation

From a signal processing point of view, averaged EEG signals could be considered as a set of mixed signals, originated from sources (or components) representing brain activities, artefacts, and measurement noise. In this methodological study, we were interested in the automatic extraction of a particular component, supposed to be the contribution of the mesial temporal source. To do that, we had to, first, separate without specific information all the components of this set (that is BSS) and second, select and validate the relevant component. This could be performed in five consecutive steps: (1) data whitening, (2) BSS, (3) ICs selection, (4) ICs labelling and (5) ICs validation (Fig. 1).

EEG datasets

As mentioned previously, we evaluated the influence, on the BSS results, of the number of EEG segments used for averaging and of the contribution of the deep source. Thus, for BSS on a specific IIS network, we made several trials with a 10-segments step of EEG signals for the average calculation. Furthermore, we considered that the contribution of the deep source could be represented by the amplitude at t_0 in the triggering SEEG signal. Therefore, to see if a few high amplitude triggering SEEG signals were sufficient to extract the deep mesial sources, we prepared two EEG datasets for each network: one with IIS sorted by decreased amplitude at t_0 in the triggering SEEG signal and the other unsorted.

Data whitening and decorrelation

Due to an insufficient spatial diversity of the EEG sensors, the EEG signals were highly correlated. Thus, the first treatment in order to guarantee the best source separation was the whitening of the EEG dataset. We have chosen to use the Zero-phase component analysis (ZCA) whitening (Bell and Sejnowski 1997) with the aim to be as close as possible (in the least squares sense) to the original observations (Kessy et al. 2018).

BSS method choice

We have chosen to use and compare three well-known and proven BSS methods implemented in many user-friendly software like EEGLAB (Delorme and Makeig 2004): infomax ICA, extended infomax ICA and JADE. Considering the estimated sources, the two first methods minimise the mutual information of these sources and the third one maximizes their non-Gaussianity. Infomax ICA is based on the information-maximization approach proposed by Bell and Sejnowski (1995) with the stochastic gradient learning rule of Amari et al. (1996). This method is effective in separating sources that have super-Gaussian distributions (sharply peaked probability density functions with heavy tails). Extended infomax ICA (Lee et al. 1999) constitute an extension of the precedent method to the separation of mixtures of super-Gaussian and sub-Gaussian sources. It uses a learning rule with a nonlinearity that considers the two kinds of distribution. JADE – joint approximate diagonalization of eigen-matrices (Cardoso and Souloumiac 1993) exploit the fourth order cumulants of the source

estimates that are a measure of non-Gaussianity. JADE seeks an orthogonal rotation of the observed mixed vectors to estimate source vectors with maximum non-Gaussianity.

Independent component selection

Scalp EEG spike is a sharply contoured waveform with a duration of 20–70 ms (Fisch 1999) and its probability density function was different of a Gaussian distribution. Then, to select the most relevant ICs representing the brain sources and thus likely to contain spikes, we have chosen to use the kurtosis value of IC as indicator. Indeed, the kurtosis could be used to appreciate the non-Gaussianity of a random variable, thus it is applied to design contrast function in BSS (Hyvärinen and Oja 1997) or to detect artefacts in EEG data (Delorme et al. 2007). In our case, we supposed that the averaged EEG signals were, as much as possible, artefact free and we just wanted to detect averaged ISS. Then, we assumed that IC containing averaged ISS was super-Gaussian with a significant positive value of the kurtosis (Fig. 2). The effect of brain sources could occur on several ICs so, to determine the relevant number of ICs to analyse, we have considered the low spatial resolution of scalp electrodes (8 to 25 electrodes for the seven patients) and some preliminary investigations that led us to select the three ICs with maximum kurtosis value, called after in decreasing order of kurtosis value, IC1, IC2 and IC3.

ICs labelling: electrode selection

For each of the selected ICs, the associate 2-D scalp map projection was obtained using the corresponding column of the inverse of the unmixing matrix issued of the BSS process. For that column, the weight with the maximum absolute value corresponded to the scalp electrode that was the most impacted by the source. This electrode was defined as scalp selected electrode for the considered IC and its name was used as a label to compare ICs.

IC waveform characterisation

The IC waveform was identified as a transient event, with one or two main peaks, distinguishable from the background activity. The earliest extremum of the IC beyond two standard deviations was taken as the extremum of the initial peak and the position of this extremum was used as a time reference, in particular to calculate the latency with respect to t_0 (Fig. 3). If there were two extrema (one maximum and one minimum), beyond two standard deviations, with a difference of more than 80 ms between them, they were considered not to be part of the same event and therefore the one with the lowest amplitude was defined as an outlier and the one with the higher amplitude was defined as the correct peak.

ICs validation

This last step concerned the validation that brain source contribution, occurring in the vicinity of the triggering SEEG contacts, was noticeable on an IC. Four criteria were used to allow this validation. First, as brain propagation is assumed to be instantaneous, if the latency between the peak position and t_0 was greater than 19.5 ms, i.e., 10 samples, this latency was not validated, and the IC was discarded. We also verified, in the same way as for IIS selection, that the amplitude of the IC at t_0 was significantly different from the amplitude of the background activity using the Walsh's test (for details see Koessler et al. 2015). Moreover, the morphologies and the scalp topographies of the IC were validated using visual expert analysis.

For easier visualisation of the final results, a bar charts representing EEG channels according to the number of selections for ICs was used for each ICi (with i = 1…3).

Influence of methodological and physiological parameters

Influence of the BSS method

First, we investigated if the choice of the BSS method had an influence on the quality of results, expressed as the validation percentage of ICs for all trials of the nine networks. Thus, the mean percentages obtained with the three methods were compared with each other, for each IC of unsorted datasets (nine tests with a sample size of nine). The H_0 hypothesis was that the medians of samples were equal and H_1 hypothesis that they were not. So, we used a two-tailed Wilcoxon rank sum test with adequate Bonferroni correction (significance level $\alpha = 0.05/9$).

Relevance of the ICs rank

We also investigated the influence of the kurtosis rank (1st, 2nd or 3rd) on the quality of results. So, we compared the mean validation percentages of IC1 with that of IC2 and IC3, for the three BSS methods and for unsorted datasets (2 × 3 tests). The H_1 hypothesis was that the median of the IC1 was greater than the median of ICi (i = 2, 3) and the H_0 hypothesis was that the median of the IC1 was not greater than the median of ICi. A one-tailed Wilcoxon rank sum test with adequate Bonferroni correction ($\alpha = 0.05/3$) was used.

Influence of the number of EEG electrodes

Another point to investigate was the influence of the number of scalp EEG electrodes on the validation percentage of ICs. For each ICi (i = 1…3), let be the dimension (27×1) vector of the mean percentage of validated ICi for the three methods (together, with all trials) and the corresponding vector of electrodes number, to appreciate the correlation between these two variables, we computed the Pearson correlation coefficient calculated on the ranks of these vectors. For some networks with the same or almost the same number of electrodes, additional approach was to evaluate the dispersion of the validation percentage of each BSS method, reflected by the corresponding standard deviation.

Contribution of the deep source

The effect of the amplitude of the deep source was evaluated by comparing, for the three BSS methods and the nine networks together, the number of validated ICs of sorted and unsorted data for the five first datasets obtained by increasing the number of EEG segments in 10-segment increments. The H_1

hypothesis was that the median of the number of validated ICs for sorted data was greater than the median of the number of validated ICs for unsorted data and the H_0 hypothesis was that the median for sorted data was not greater than the median for unsorted data. The comparison between the obtained 5-item samples was realised with a one-tailed Wilcoxon rank sum test. As additional information, the mean values of triggering SEEG signal for the first trial and the 5th trial were also collected, for both sorted and unsorted data.

Evolution of the validation percentage of ICs according to the number of averaged EEG segments

Furthermore, we evaluated, for all trials and for the three BSS methods, the minimum number of EEG segments from which the different ICs can be validated. Next, we analysed the graphs of the evolution of the validation percentage of ICs according to the number of segments to find out if there were some specific patterns. Finally, we identified the cases of simultaneous validation of two or three ICs for the same trial.

Causes of non-validation of ICs and associated indicators

We tried to identify and quantify the different causes of non-validation of the first three ICs using relevant indicators. These causes could be: (i) the presence of an artefact on EEG signals that induces an abnormal pattern on ICs that was mistaken for a spike, inaccurate estimation of the t_0 for some segments, time difference between the deep source and the corresponding SEEG triggering signal which increases latency with respect to t_0, (ii) noise level too high to detect the correct peak at t_0, (iii) presence of a second deep source or artefact that leads to an incorrect cartography. An excessive latency value may indicate the presence of one of the first set of causes or a high level of noise. If the latency was correct, non-detection using the Walsh's test may indicate a slight peak shift due to inaccurate estimation of t_0 or time difference between the deep source and the triggering signal and, at last, if the peak amplitude was validated, an incorrect cartography could suggest the presence of another source or artefact. Then, we listed, for all the non-validation, the latency, the result of amplitude Walsh's test and of cartography validation to build a table showing the percentage of non-detection of ICs according to the value of these three indicators. In this table, the latency evaluation was split up into four cases: latency greater than 250 ms, latency between 250 and 100 ms, latency between 100 and 50 ms and latency between 50 and 20 ms.

Results

Patient networks characterisation

For all seven patients, nine M networks were validated (Table 1). These networks included sources localized in the anterior hippocampus, six included sources localized in the middle and/or posterior hippocampus, seven in the amygdala, and five in the para-hippocampal gyrus (Koessler et al. 2015). For these networks, a total of 1,949 IIS was selected. The mean IIS amplitude was 729±279 μV.

Table 1
Epileptonic zone definition and anatomical distribution of the interictal spikes for each mesial spike network for all patients

Patients	Epileptogenic zone defined by SEEG	Laterality	IIS networks	Numbers of IIS	Int. Amy – MTG	Int. Ant. Hipp – int. ant. MTG	Int.Post. Hipp – int. post. MTG	Int. Parahipp – int. basal T	Int. Mid. Hipp – int. basal T
P1	Mesial	R + L	1	272	×	0			×
			2	149	×	×		0	
P2	Mesial, pole	R	3	440	×	×	×	0	
P3	Mesial	L	4	171	×	0		×	×
			5	94	×	×	0		×
P4	Mesial	L	6	159	×	×		0	×
P5	Mesial, pole	L	7	368	×	×	×		0
P6	Mesial, ant. and mid. basal part	L	8	248		0			
P7	Mesial, pole, insula	R	9	48	×	0		×	

"×" indicates the presence of epileptic spikes with SNR ≥ 2 and bold circles indicate for the spikes serving as triggers for averaging. *Int.* internal, *Amy* amygdala, *MTG* middle temporal gyrus, *Hipp* hippocampus, *Parahipp* para-hippocampal, *T* temporal, Basal temporal corresponded to fusiform gyrus or inferior temporal gyrus, *L* left, *R* right, Ant. Anterieur, Int. internal, Mid. Middle, Lat. Lateral

According to this dataset, the corresponding number of trials was equal to 195 for the nine networks with a mean number of trials per network equal to 21.7 (min: 5, max: 44).

Overview of the results for all trials together

For all nine networks (195 trials) and the three BSS methods together, that is for a total of 585 results, the percentages of validated IC1, IC2 and IC3 were 53%, 8% and 3% for unsorted data respectively.

For all nine networks, the sums of overall mean percentage of all validated ICs (i.e., IC1 + IC2 + IC3) for infomax ICA, extended infomax ICA and JADE methods were 61%, 53% and 62% respectively. The grand mean percentages of validated IC1, IC2 and IC3 for the three BSS methods together were 49 ± 35%, 7 ± 6% and 3 ± 4% for unsorted data respectively. More specifically, for infomax ICA method, the overall mean percentages of validated IC1, IC2 and IC3 were 49 ± 34%, 7 ± 10% and 5 ± 8% respectively; for extended infomax ICA these numbers were 46 ± 38%, 6 ± 3% and 2 ± 2% and for JADE method they were 52 ± 34%, 8 ± 10% and 3 ± 4% (Table 2 and Fig. 4).

Table 2
Validation percentages of ICs for the whole set of trials of each network according to each blind source separation method and for sorted and unsorted

Patients	IIS networks	No. of surface electrodes	No. of trials	% of validation of IC1 for the three BSS methods						% of validation of IC2 for the three BSS methods						% of validation methods	
				Infomax ICA		Extended infomax ICA		JADE		Infomax ICA		Extended infomax ICA		JADE		Infomax ICA	
				Sor. data set	Uns. data set	Sor. data set	Uns. data set	Sor. data set	Uns. data set	Sor. data set	Uns. data set	Sor. data set	Uns. data set	Sor. data set	Uns. data set	Sor. data set	Uns. data set
P1	1	8	27	33	70	41	78	41	81	33	19	30	4	26	7	0	15
	2		15	100	100	87	93	100	93	0	0	13	7	0	7	0	0
P2	3	25	44	66	66	77	73	75	68	27	18	9	5	16	16	5	0
P3	4	13	17	88	65	82	76	88	76	12	0	24	6	6	6	0	0
	5		9	44	67	67	56	33	56	56	0	22	11	67	0	0	0
P4	6	13	16	6	25	0	0	25	31	19	25	6	6	13	31	13	19
P5	7	14	37	16	49	24	35	32	62	0	0	11	8	8	5	0	0
P6	8	12	25	8	0	12	0	8	0	28	4	28	4	28	0	0	8
P7	9	20	5	0	0	0	0	0	0	0	0	0	0	0	0	0	0

Sor. Sorted, *Uns.* Unsorted; BSS. Blind source separation; IIS. Intracerebral Interictal spikes., IC. Independent component

At last, for all nine networks and the three BSS methods (27 results), the total percentage of cases without any validated IC for IC1, IC2 and IC3 were 26%, 33% and 63% for unsorted data respectively.

Considering now each network separately, for the three ICs with the three BSS methods and for unsorted data (9 combinations), there is only one network (i.e., #9) without any validated IC. For the other networks, the percentage of results without validated IC varied from 11 to 55% (Table 2).

The analysis of the bar charts representing EEG channels according to the number of selections for ICs showed that, for IC1, the patterns were different between networks with high and low validation percentage for ICs (Fig. 5). Thus, for bar charts with high validation percentage, the selected electrode was often the same, inducing a large bar for this electrode and few smaller ones for the other electrodes (Fig. 5a, networks 1 to 5 and 7) whereas, for low validation percentage bar charts, the range of bar amplitudes was lower and, often, the number of bars was higher (Fig. 5a, networks 6, 8 and 9). On the contrary, for IC2, there was no clear pattern to differentiate between bar charts (Fig. 5b), as well as IC3.

Influence of methodological and physiological parameters

Influence of the BSS method

The mean p-value for the nine comparison tests between the BSS methods was equal to 0.83 ± 0.20 with a minimum p-value equal to 0.44. Consequently, H_0 hypothesis (equality of medians) could not be rejected for these nine tests. Consequently, there is no significant influence of the BSS method for the extraction of deep mesial sources.

Relevance of the ICs rank

For infomax ICA, extended infomax ICA and JADE methods, the p-values for the comparison tests between the mean validation percentages of IC1 and IC2 were 0.0067, 0.0986, 0.0126 respectively. In the same way, the p-values for the comparison tests between the mean validation percentages of IC1 and IC3 were 0.0034, 0.0263, 0.0054 respectively. Consequently, H_1 hypothesis (median of IC1 > median of ICi for i = 2, 3) could be accepted for infomax ICA and JADE methods.

Influence of the number of EEG electrodes

For IC1, IC2 and IC3, the Pearson correlation coefficients between the vector of mean percentage of validated IC for the three methods and the corresponding vector of electrodes number, were − 0.36, 0.05 and − 0.04 respectively. For all these coefficients, the corresponding p-value was greater than 0.05 indicating that the H_0 hypothesis (correlation is zero) could not be rejected. Networks 4 to 8 had a number of electrodes between 12 and 14 with 9 common electrodes, so we computed the corresponding standard deviation of the validation percentage of each BSS method. For infomax ICA, extended infomax ICA and JADE

methods and for IC1, the standard deviations were 29%, 34% and 30% respectively; for IC2, standard deviations were 11%, 3% and 13% respectively and for IC3, 8%, 3% and 6% respectively. Figure 6 shows the validation percentage values obtained for the JADE method alone.

Contribution of the deep source

For trials one to five, the number of validated ICs was 10, 13, 13, 15 and 15 (total = 66) for sorted data respectively and 1, 6, 7, 10 and 13 (total = 37) for unsorted data respectively. For these five first datasets, the p-value of the comparison test between the number of validated ICs for both sorted and unsorted data was 0.03. Consequently, H_1 hypothesis (median of validated ICs for sorted data > median of validated ICs for unsorted data) could be accepted. As an illustration, Fig. 7, networks 2 to 6, showed that, for the five first trials, the validation percentage of ICs was better for sorted data than for unsorted data. Next, for the first trial and for sorted data, five networks had one validated IC for at least one method and, for these networks (2, 3, 4, 5 and 9), the means of the triggering SEEG signal were 698 µV, 2,022 µV, 1,574 µV, 920 µV, and 757 µV respectively. For the first trial and for unsorted data, the network 2 had one validated IC and, for this network, the mean of the triggering SEEG signal was 359 µV. At last, for the 5th trial, the mean of the triggering SEEG signals for all networks were 1,085 and 652 µV for sorted and unsorted data respectively.

Evolution of the validation percentage of ICs according to the number of averaged EEG segments

The mean values of the minimum number of segments when IC1, IC2 and IC3 were validated for the first time were 70 ± 77, 71 ± 63 and 67 ± 50 for sorted data respectively and 62 ± 41, 80 ± 56 and 129 ± 58 for unsorted data respectively. The evolution curves of the validation percentage of ICs as a function of the number of EEG segments can be classified into four main categories: (1) curves for which, after a minimum number of segments, the validation percentage increases almost all the time, (2) curves with alternating increases and decreases, (3) curves with one-time increase, (4) curves with a validation percentage always equal to zero (Fig. 7). The first category concerned exclusively some IC1s and indicated that, for the corresponding networks, the deep brain source was detectable in almost all cases after a minimum number of segments (Fig. 7, networks 1 to 4 and 7). The second category involved IC1s and IC2s whose evolutions appeared to be coupled (one IC increases and the other decreases) as if the brain source contribution was identified by one IC and then by another ("switching effect") (Fig. 7a, network 5 and Fig. 7b, network 6). Notice that this change can also be observed at the beginning of some curves of the previous category (Fig. 7, networks 1 and 3). The third category concerned IC2s (Fig. 7, network 4, Fig. 7b, networks 1, 2 and 7), mainly IC3s (Fig. 7, networks 3 and 8, Fig. 7a, networks 4 and 6) and rarely IC1 (Fig. 7a, network 8). The last category concerned IC1 (Fig. 7, network 9), IC2 (Fig. 7, networks 2 and 9, Fig. 7b, networks 5 and 8) and mainly IC3 (Fig. 7, networks 2, 5, 7 and 9, Fig. 7a, network 1, Fig. 7b, network 4).

For the total number of trials (1170) obtained for the three BSS methods and both sorted and unsorted data, the percentage of trials with two ICs validated at the same time was 1.5%. These trials concerned networks 1, 2, 4 and 8 with concordant selected electrodes. Note that this result was consistent with the "switching effect" described above.

Causes of non-validation of ICs and associated indicators

For the three ICs with the three BSS methods and unsorted data, the percentages of non-validation associated to Walsh's test and cartography validation were very stable with mean about 7 ± 2% and 5 ± 2% respectively. By contrast, the percentages of non-validation associated to the four categories of latency defined above were increasing for IC2 (77%) and IC3 (87%) comparing with IC1 (42%) (Table 3). For IC1 specifically, the cases of incorrect latency were different according to the networks. Thus, for networks 1 to 4, the mean of incorrect latencies was equal to 15%; they were mostly higher than 250 ms and appeared when the number of averaged EEG segments was low, suggesting that source separation was not yet conclusive, or punctually at any time, due to EEG artefact. Next, for networks 5 and 7, the mean of incorrect latencies was equal to 37%; they were mainly associated with a low number of averaged EEG segments and all categories of latencies were concerned even if these latencies were often comprised between 20 and 50 ms as if the IC waveform was trying to synchronize to t_0 without success. Lastly, for networks 6, 8 and 9, the mean of incorrect latencies was equal to 82% and all the categories of incorrect latencies were concerned.

Table 3
Mean non-validation percentages of ICs, for the whole set of trials and for unsorted sets of EEG recordings, according to latency value, Walsh's test result and cartography validation

	IC1	IC2	IC3
|Lat.| > 250 ms	17	26	33
250 > |Lat.| > 100 ms	8	23	26
100 > |Lat.| > 50 ms	3	7	13
50 > |Lat.| > 20 ms	14	22	16
Amplitude rejected	4	8	7
Cartography rejected	4	7	3
Total	51	93	97

Lat. Latency; IC: independent component

Improvement of the extraction: BSS analysis with expert control

According to the causes of non-validation, two improvements could be suggested to ameliorate the validation percentage of ICs. First, the use of a minimum number of average EEG segments, greater than the minimum observed mean values (e.g., 100 segments), could improve the extraction of the ICs. Second, when the peak latency of the IC1 was too long (e.g., greater than 250 ms in absolute value), it clearly indicates the presence of some artefacts or noise in the scalp EEG signals. So, replacing this IC1 by the corresponding IC2 and this IC2 by the corresponding IC3 could also improve the extraction. Consequently, the IC3 data were incomplete and IC3 could no longer be used for various comparisons. This situation would not be an important problem because, in this study, its validation percentage was very low. For all initial trials with the three methods, when this solution was applied, the substitution involved 79 IC1 (14%) and the proportion of these IC1 that were replaced by an IC2 with a correct latency was 41%.

With these two improvements under visual expertise, two networks with insufficient number of segments (networks 5 and 9) were discarded. The total number of trials was then equal to 118. For all seven networks, the mean percentage of validated IC1 and IC2 for the three methods together were 70 ± 35% and 8 ± 6% for unsorted data respectively. More specifically, the overall mean percentage of validated IC1 and IC2 were 69 ± 34% and 14 ± 18% respectively for infomax ICA method, 60 ± 45% and 6 ± 8% respectively for extended infomax ICA and 80 ± 36% and 4 ± 5% respectively for JADE. Then, the sums of overall mean percentage of validated ICs for infomax ICA, extended infomax ICA and JADE methods were 83%, 66% and 84% respectively (Fig. 8).

BSS analysis under visual expertise resulted in validated IC1 associated with a relevant selected electrode for all networks with all methods (7 networks × 3 methods: 21 cases), except for network 6 (validation percentage equal to zero for extended infomax ICA), network 7 (validation percentage equal to 46% for extended infomax ICA) and network 8 (validation percentage equal to zero for all methods) (Fig. 9 and Fig. 10).

As before, the twelve comparison tests of BSS methods (three methods compared with each other, for two IC and for two datasets) applied to the results of these improvements concluded that H_0 hypothesis (equality of medians) could not be rejected and thus the BSS methods remained equivalent (mean p-value equal to 0.55 ± 0.24 with a minimum value equal to 0.1538). Conversely, the three comparison tests between mean validation percentage of IC1 and IC2 concluded that H_1 hypothesis (median of IC1 > median of IC2) could be accepted for the Infomax ICA and JADE methods (for infomax ICA, extended infomax ICA and JADE methods, the p-values were 0.0058, 0.0294, 0.0047 respectively). Next, for the correlation between mean percentage of validated IC and electrodes number, the H_0 hypothesis (correlation is zero) could not be rejected (for IC1 and IC2, the p-value was greater than 0.05 and the Pearson correlation coefficient was respectively equal to -0.13 and 0.16). Lastly, for networks 4 and 6 to 8 with a number of electrodes between 12 and 14, the standard deviations of the validation percentage for infomax ICA, extended infomax ICA and JADE methods, were 41%, 42% and 48% for IC1 respectively and 16%, 8% and 4% for IC2 respectively.

Discussion

Funding and Statements

This study was funded by the French National Research Agency (ANR, France Relance) (BioNumMA). The authors have no relevant financial or non-financial interests to disclose. The datasets generated during and/or analyzed during the current study are not publicly available for ethical reasons but are available from the corresponding author on reasonable request.

Conclusion

Having established the contribution of deep mesial temporal sources to scalp EEG (Koessler et al. 2015), we demonstrated in this methodological study that the automatic extraction of these invisible sources on the scalp is possible under certain conditions. The first independent component extracted from the scalp EEG signals was validated in mean from 46–80% according to the different parameters. Despite the unperfect detection, this study shows that a relatively simple signal analysis of scalp EEG can extract epileptic discharges of brain sources that are hidden/mixed with others and so, can escape to visual expert analysis. For the clinical diagnosis of epilepsy, this solution that relies on non-invasive recordings would be important because it can change the medical care, especially in drug resistant epilepsy where source detection and localization (e.g., deep and/or lateral) are crucial. Finally, it is important to mention that we have deliberately used common available toolboxes to test their performances and finally found promising results. These offer several interesting perspectives for the development of new signal processing tools and methods that could improve the performance of deep source extraction.

Abbreviations

BSS Blind source separation

EEG Electroencephalography

IC Independent component

ICA Independent component analysis

IIS Interictal Intracerebral spike

ISS Interictal Surface Spike

MEG Magnetoencephalography

MTL Mesial temporal lobe

NC Neocortical

SEEG Stereoelectroencephalography

SNR Signal to noise ratio

TLE Temporal lobe epilepsy

Declarations

Funding and Statements

This study was funded by the French National Research Agency (ANR, France Relance) (BioNumMA). The authors have no relevant financial or non-financial interests to disclose. The datasets generated during and/or analyzed during the current study are not publicly available for ethical reasons but are available from the corresponding author on reasonable request.

References

1. Akhtari M, Bryant HC, Mamelak AN, Flynn ER, Heller L, Shih JJ, et al. (2002) Conductivities of three-layer line human skull. Brain Topogr 14:151-167. https://doi.org/10.1023/A:1014590923185
2. Amari S, Cichocki A, Yang HH (1996) A New Learning Algorithm for Blind Signal Separation. Advances in Neural Information Processing Systems 8:757-763. https://proceedings.neurips.cc/paper/1995/file/e19347e1c3ca0c0b97de5fb3b690855a-Paper.pdf
3. Bell AJ, Sejnowski TJ (1995) An information-maximization approach to blind separation and blind deconvolution. Neural Comput 7:1129-1159. https://doi.org/10.1162/neco.1995.7.6.1129
4. Bell AJ, Sejnowski TJ (1997) The “independent components” of natural scenes are edge filters. Vis Res 37:3327-3338. https://doi.org/10.1016/S0042-6989(97)00121-1
5. Bourien, J., Bartolomei, F., Bellanger, J. J., Gavaret, M., Chauvel, P., & Wendling, F. (2005). A method to identify reproducible subsets of co-activated structures during interictal spikes. Application to intracerebral EEG in temporal lobe epilepsy. *Clinical Neurophysiology*, *116*(2), 443-455. https://doi.org/10.1016/j.clinph.2004.08.010
6. Cardoso JF, Souloumiac A (1993) Blind Beamforming for non-Gaussian Signals. IEE Proc-F 40:362-370. https://doi.org/10.1049/ip-f-2.1993.0054
7. Congedo M, Gouy-Pailler C, Jutten C (2008) On the blind source separation of human electroencephalogram by approximate joint diagonalization of second order statistics. Clin Neurophysiol 119:2677-2686. https://doi.org/10.1016/j.clinph.2008.09.007
8. Delorme A, Makeig S (2004) EEGLAB: an open source toolbox for analysis of single-trial EEG dynamics including independent component analysis. J Neurosci Methods 134:9-21. https://doi.org/10.1016/j.jneumeth.2003.10.009
9. Delorme A, Sejnowski T, Makeig S (2007) Enhanced detection of artifacts in EEG data using higher-orderstatistics and independent component analysis. Neuroimage 34:1443-1449. https://doi.org/10.1016/j.neuroimage.2006.11.004
10. Fisch BJ (1999) Fisch and Spehlmann’s EEG Primer, basic principles of digital and analog EEG. 3rd Ed Elsevier
11. Hyvärinen A, Oja E (1997) A fast fixed-point algorithm for independent component analysis. Neural Comput 9:1483-1492. https://doi.org/10.1162/neco.1997.9.7.1483
12. Jung TP, Makeig S, McKeown MJ, Bell AJ, Lee TW, Sejnowski TJ (2001) Imaging brain dynamics using independent component analysis. Proc IEEE 89:1107-1122. https://doi.org/10.1109/5.939827
13. Jutten C, Karhunen J (2004) Advances in blind source separation (BSS) and independent component analysis (ICA) for nonlinear mixtures Int J Neural Syst 14:267-92. https://doi.org/10.1142/s012906570400208x
14. Karunakaran, S., Rollo, M. J., Kim, K., Johnson, J. A., Kalamangalam, G. P., Aazhang, B., & Tandon, N. (2018). The interictal mesial temporal lobe epilepsy network. Epilepsia, 59(1), 244-258. https://doi.org/10.1111/epi.13959
15. Kessy A, Lewin A, Strimmer K (2018) Optimal whitening and decorrelation. The American Statistician 72:309-314. https://doi.org/10.1080/00031305.2016.1277159
16. Koessler L, Cecchin T, Colnat-Coulbois S, Vignal JP, Jonas J, Vespignani H, Ramantani G, Maillard LG (2015) Catching the invisible: mesial temporal source contribution to simultaneous EEG and SEEG recordings. Brain Topogr 28:5-20. https://doi.org/10.1007/s10548-014-0417-z
17. Lee S, Wu S, Tao JX, Rose S, Warnke PC, Issa NP, van Drongelen W (2021) Manifestation of Hippocampal Interictal Discharges on Clinical Scalp EEG Recordings. J Clin Neurophysiol, published ahead-of-print 14 may 2021. https://doi.org/10.1097/wnp.0000000000000867
18. Lee TW, Girolami M, Sejnowski TJ (1999) Independent component analysis using an extended infomax algorithm for mixed sub-Gaussian and super-Gaussian sources. Neural Comput, 11:409-433. https://doi.org/10.1162/089976699300016719
19. Pizzo F, Roehri N, Medina Villalon S, Trébuchon A, Chen S, Lagarde S, Carron R, Gavaret M, Giusiano B, McGonigal A, Bartolomei F, Badier JM, Bénar CG (2019) Deep brain activities can be detected with magnetoencephalography. Nat Commun 10:971. https://doi.org/10.1038/s41467-019-08665-5
20. Pyrzowski J, Le Douget JE, Fouad A, Siemiński M, Jędrzejczak J, Le Van Quyen M (2021) Zero-crossing patterns reveal subtle epileptiform discharges in the scalp EEG. Sci Rep 11:4128. https://doi.org/10.1038/s41598-021-83337-3

21. Ramantani G, Maillard L, Koessler L (2016) Correlation of invasive EEG and scalp EEG. Seizure 41:196-200. https://doi.org/10.1016/j.seizure.2016.05.018
22. Seeck M, Koessler L, Bast T, Leijten F, Michel C, Baumgartner C, He B, Beniczky S (2017) The standardized EEG electrode array of the IFCN. Clin Neurophysiol 128: 2070-2077. https://doi.org/10.1016/j.clinph.2017.06.254

Figures

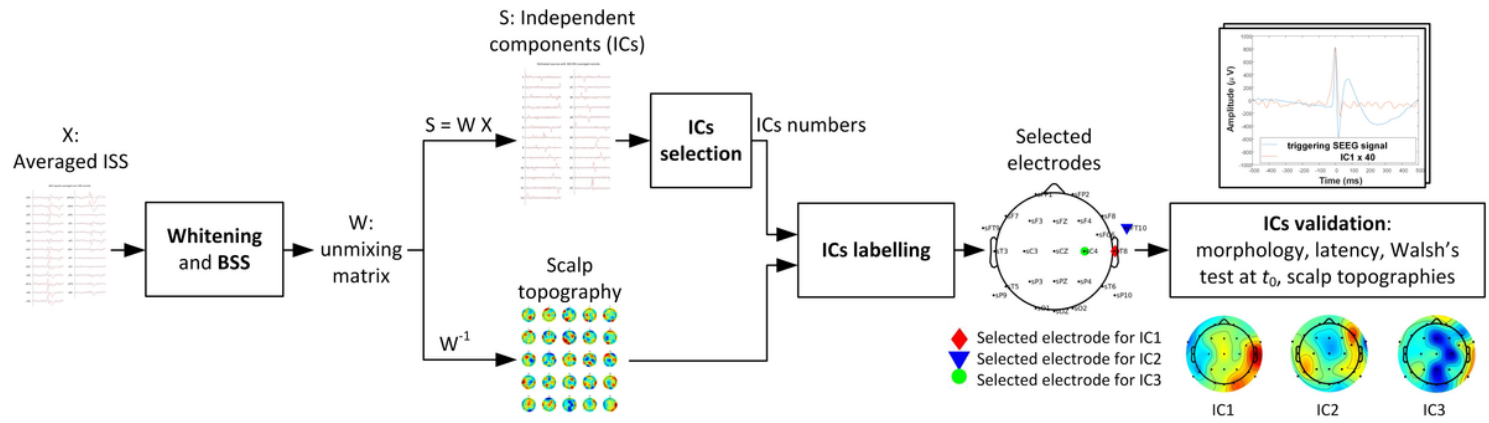

Figure 1

Overview of blind source separation and independent components validation. *ISS* Interictal surface spike; ICs: Independent components; BSS: Blind source separation

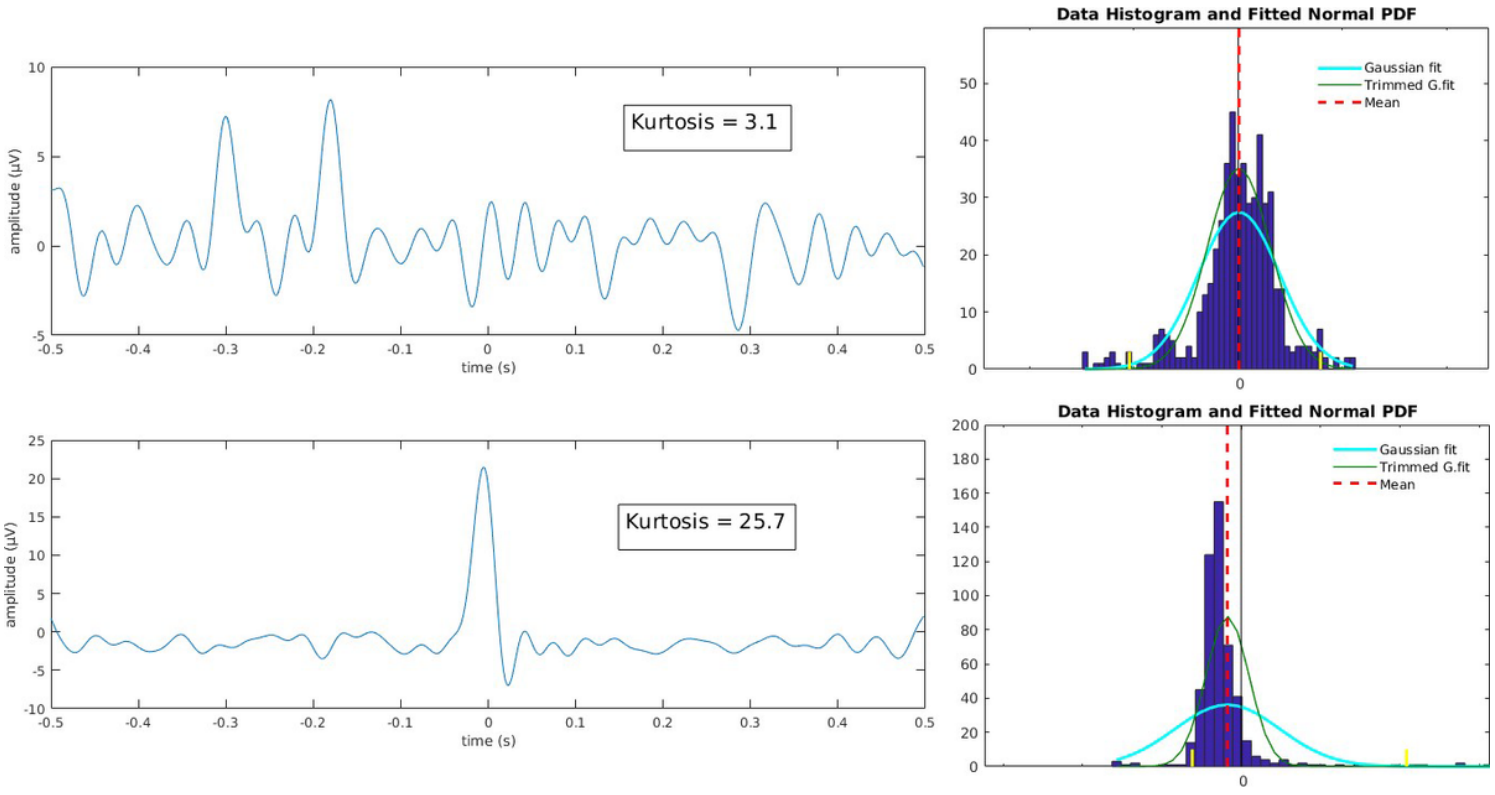

Figure 2

Example of kurtosis values and distribution of two ICs obtained for patient 2, network 3. The upper example is near to Gaussian whereas the lower is super-Gaussian (sharply peaked probability density functions with heavy tails)

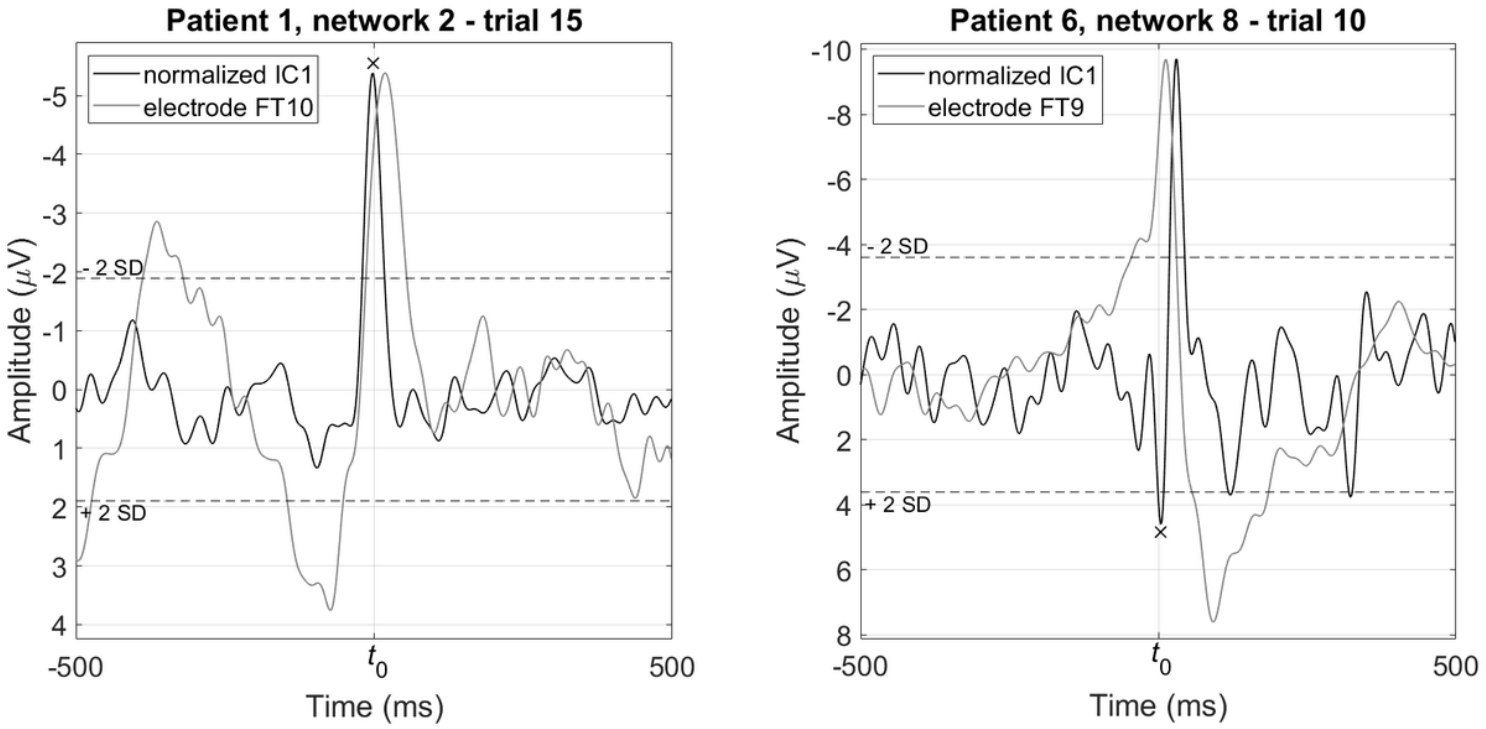

Figure 3

Example of IC1s with the Infomax ICA method, associated with the mean value of the selected electrode signal. For viewing, normalisation consists of adapting the amplitude of the IC to that of the selected electrode signal and the cross indicates the extremum used to compute the latency. IC: Independent component.

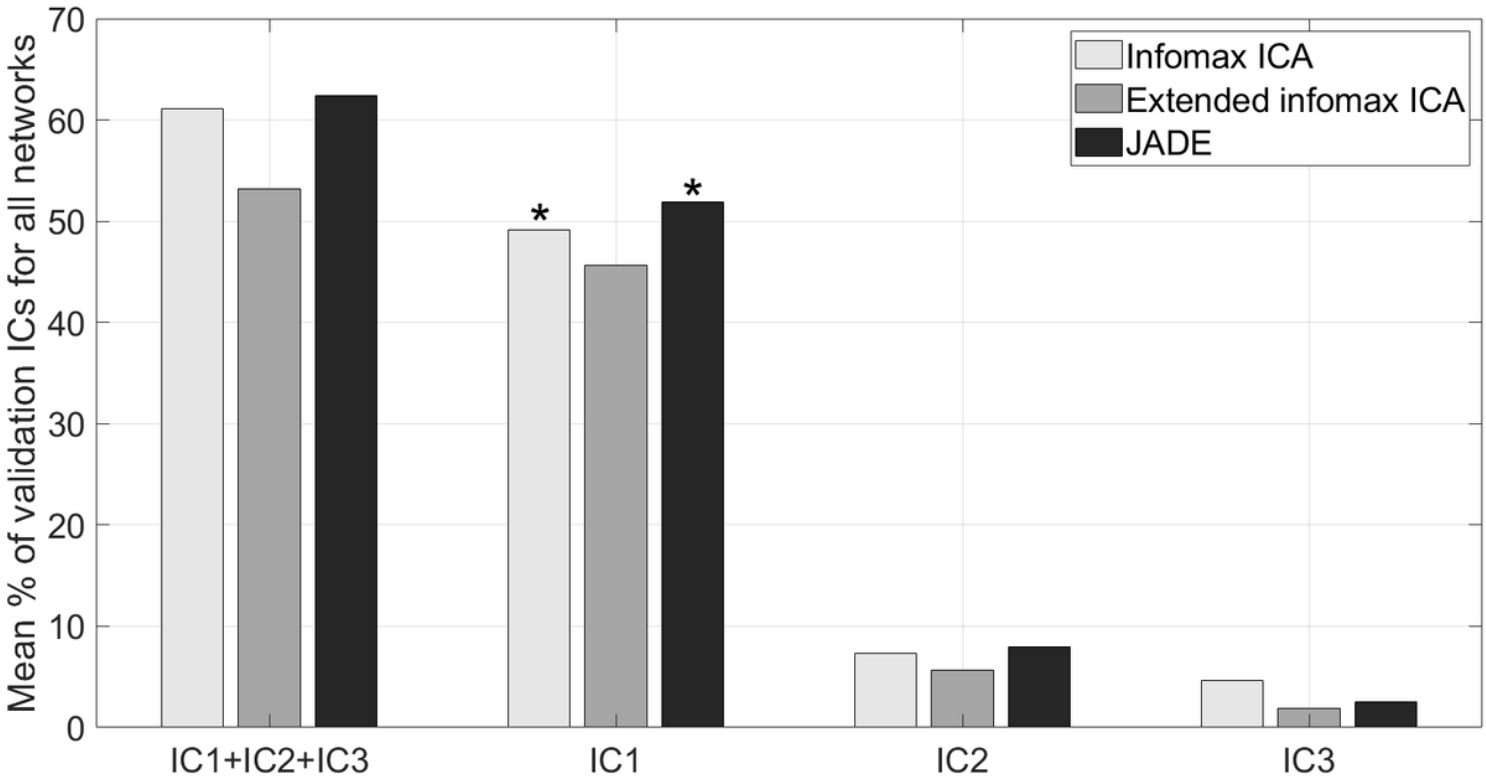

Figure 4

Mean validation percentage of ICs and their sum for all networks and all patients. The stars indicate a significant difference between the medians of IC1 with IC2 and IC3.

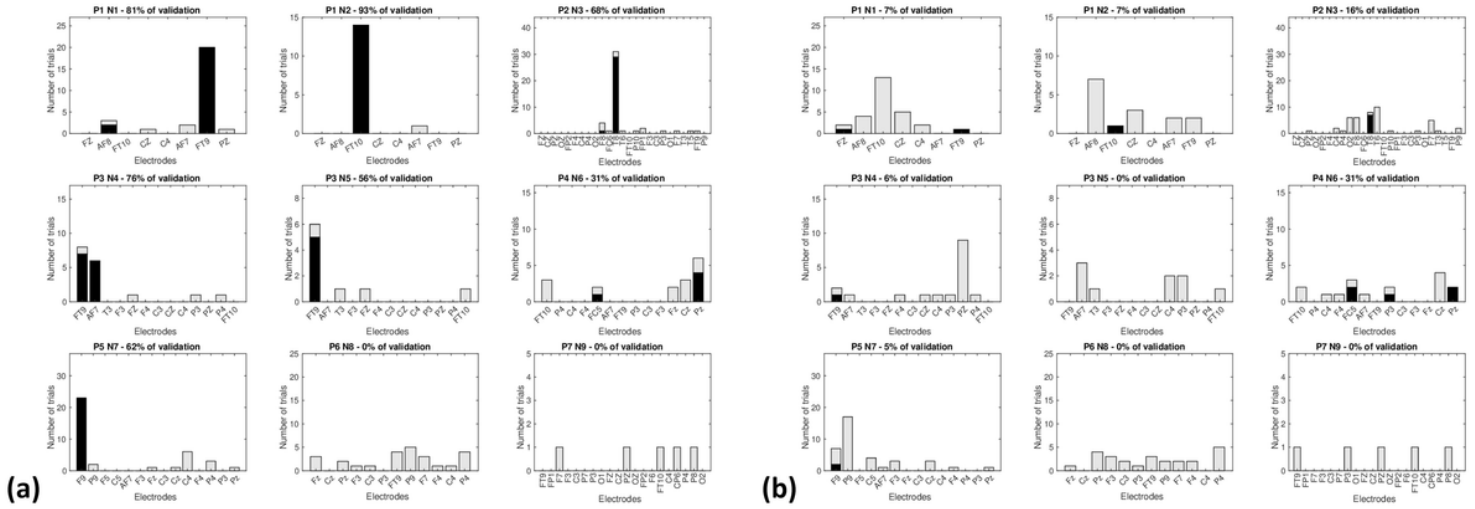

Figure 5

Classification, for the JADE method with all trials and the unsorted data, of EEG channels according to the number of selections for ICs. **a** IC1. **b** IC2. The *black bar* and the *grey bar* correspond to validated and non-validated ICs respectively, *P* Patient, *N* Network

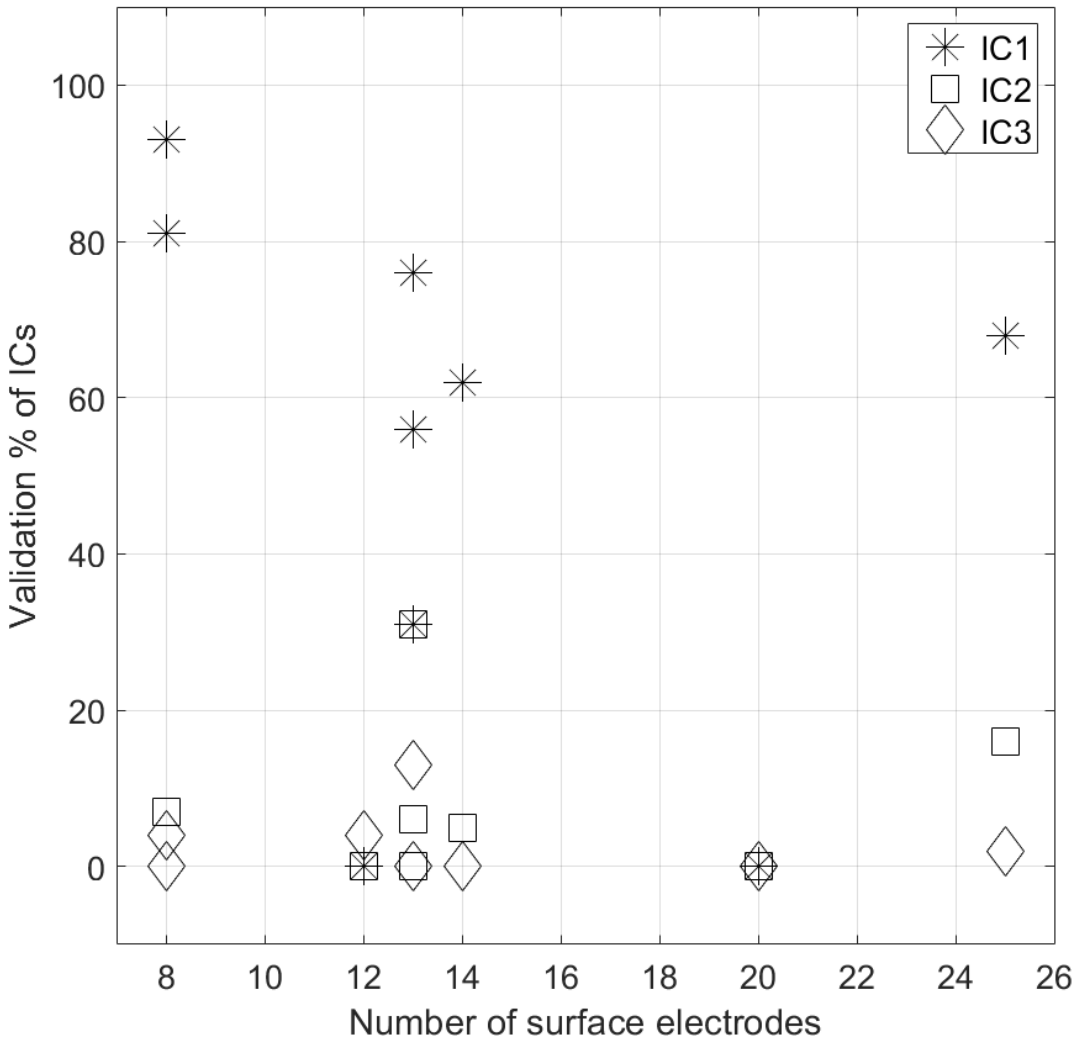

Figure 6

Validation percentage of ICs, for the nine networks, according to the number of surface electrodes using the JADE method with all unsorted trials

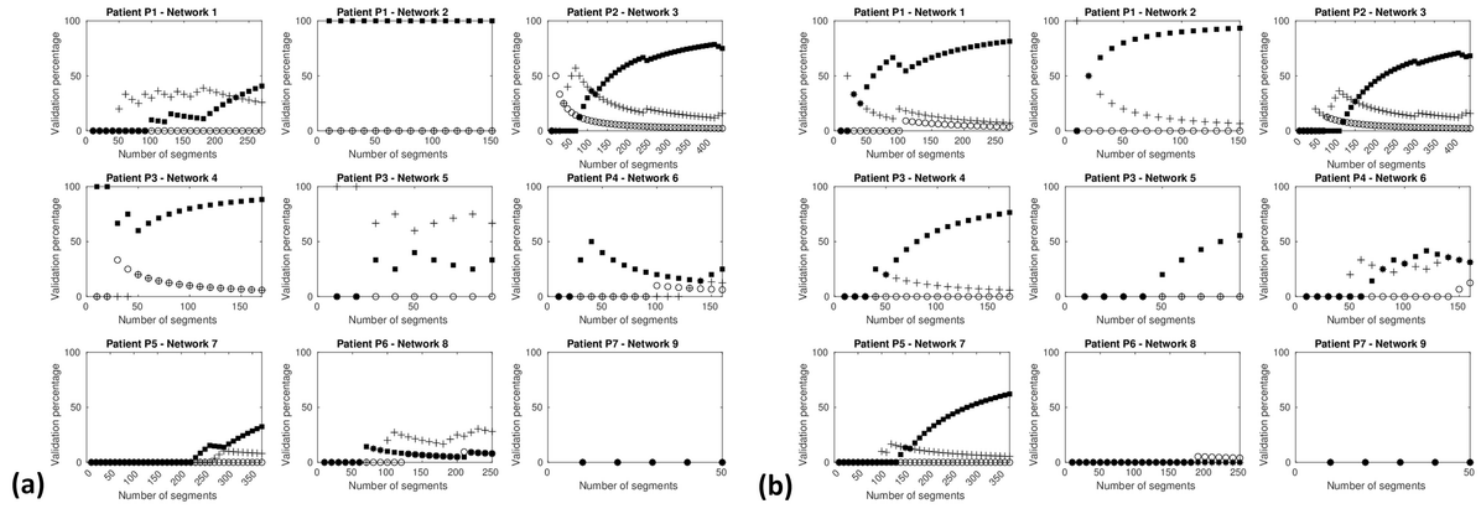

Figure 7

Evolution of the validation percentage of ICs according to the number of segments for the JADE method. **a** Sorted data. **b**Unsorted data. The *square*, the *cross* and *the circle* corresponded to IC1, IC2 and IC3 respectively.

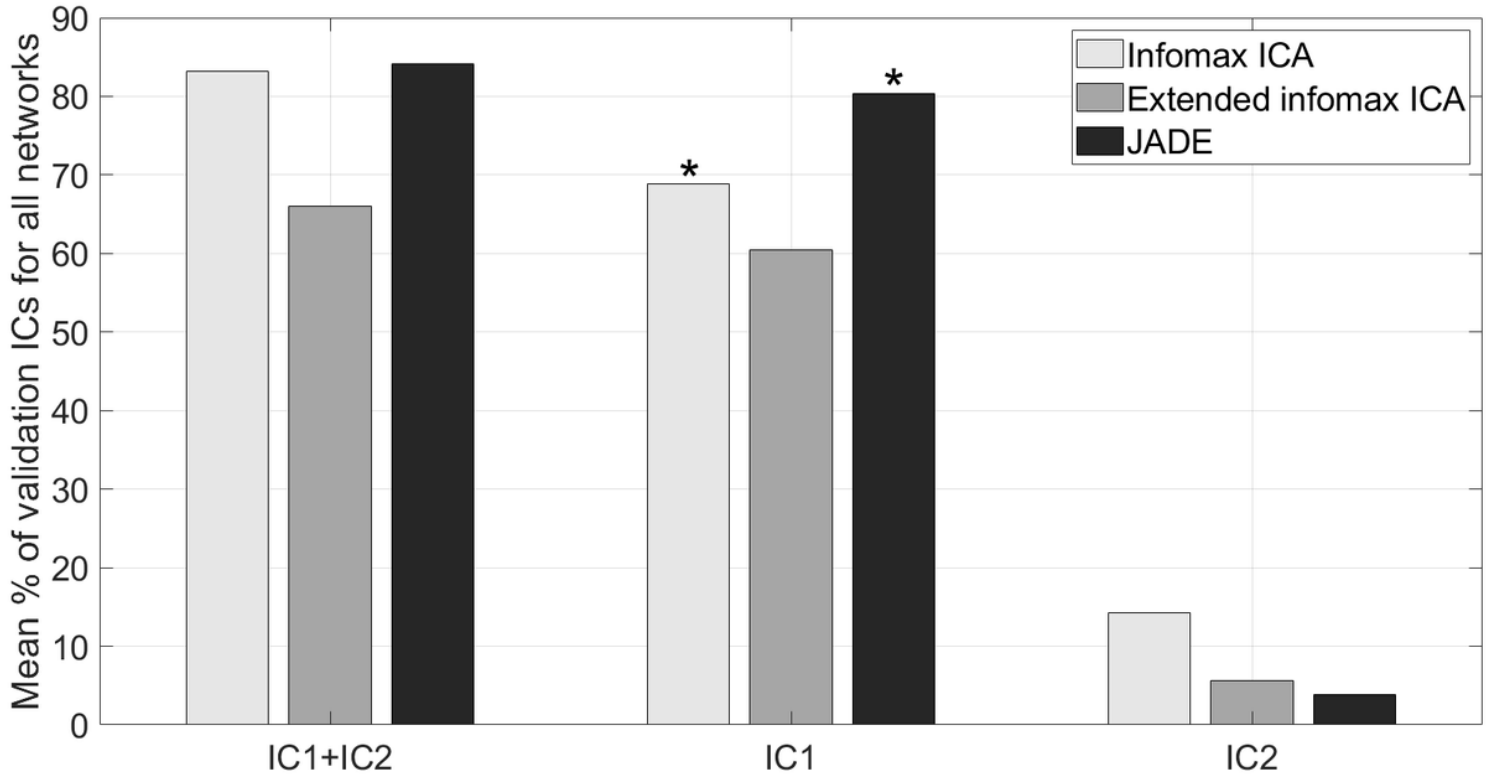

Figure 8

BSS analysis with expert control: mean validation percentage of IC1 and IC2 for networks 1 to 4 and 6 to 8 and their sum. The stars indicate the validation of the hypothesis that the median of IC1 was greater than the median of IC2

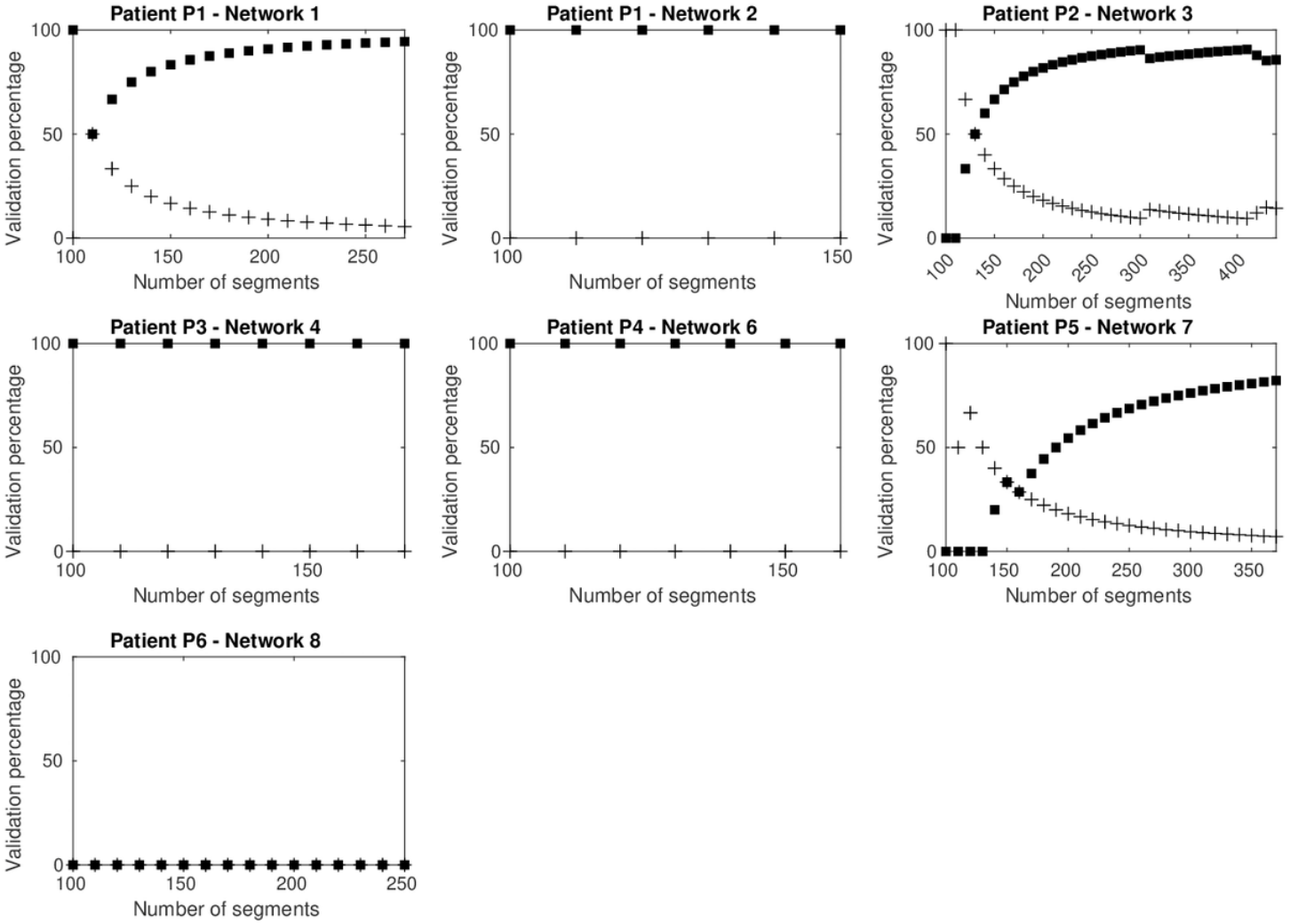

Figure 9

BSS analysis with expert control: evolution, for the JADE method, of the validation percentage of IC1 and IC2 according to the number of segments for unsorted data. The *square* and the *cross* correspond to IC1 and IC2 respectively

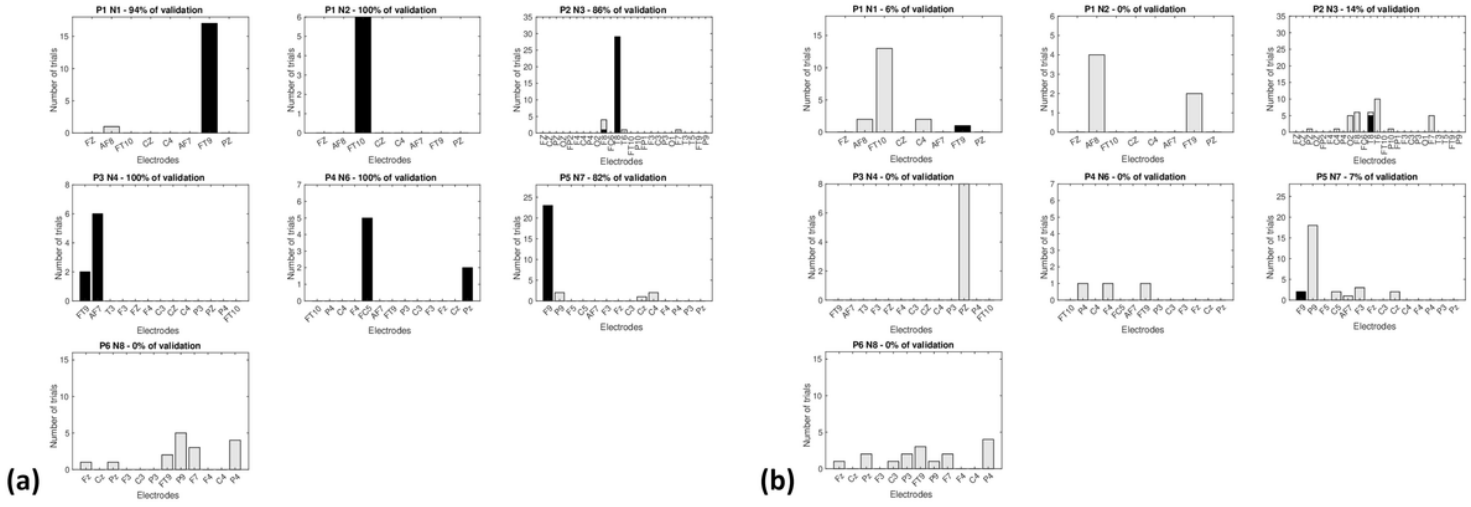

Figure 10

Blind source separation analysis with expert control: classification, for the JADE method with all trials and for unsorted data, of EEG channels according to the number of selections for ICs. **a** IC1. **b** IC2. The *black bar* and the *grey bar* correspond respectively to validated and non-validated ICs, *P* Patient, *N* Network